

LENDING COPY

102523-1002



DNPL EL/TM.016

THE N.I.N.A. POLE FACE WINDINGS

by

DR. N.R.S. TAIT.

National Institute for Research
in Nuclear Science.

Daresbury.

January, 1964.

<u>Contents.</u>	<u>Page</u>
1. Introduction.	2
2. Continuous Current Distributions.	4
3. Calculation of Conductor Positions.	6
4. Calculation of Conductor Field Distribution.	7
5. Comparison of Ideal and Real Fields.	11
6. Non-Hyperbolic Pole Faces.	12
7. Induced E.M.F. and Forces.	14
8. The Sextupole Field.	15
9. Numerical Results.	17
10. Excitation of the Windings.	25
11. References.	25
12. Acknowledgments.	25

THE N.I.N.A. POLE FACE WINDINGS.1. Introduction.

It is necessary to make small modifications to the magnetic field of the synchrotron magnets. These are achieved by the use of pole-face windings which are current-carrying wires situated on the pole faces of the magnets and directed along the length of the magnets.

The modifications to the field are only needed during and for a short time after injection of the electron beam, when the main field is low (~ 64 gauss).

At moderate field strengths (3 - 5 kilo-gauss), the variation of the field index $n = -\frac{r_0}{B_0} \frac{dB}{dr}$ with radial position on the median plane can be predicted theoretically (1). The pole faces have been designed to keep n within $\pm 1\%$ of the ideal value n_0 for both F and D magnets at these field strengths. It can be seen from Fig. 1 that the field index is well within the 1% limits except at points at the extreme ends of the working region.

Measurements of the field index for the DESY magnets (2) give good agreement with the calculated values.

1.1. Correction of the Field at Low Field Strengths.

At low field strengths the field index is considerably altered, mainly because of the effects of remanence in the magnet core.

The field at a point in the median plane is

$$B_t = B + B_r$$

where B = main field

and B_r = remanent field

hence

using the expression $n = -\frac{r_0}{B_0} \frac{dB}{dr}$,

$$n_t = n_0 \frac{B_0}{B_{t0}} + n_r \frac{B_r}{B_{t0}} \quad (1)$$

where $B_{t0} = B_0 + B_{r0}$ = field on the equilibrium orbit.

At moderate values of B_0 , $B_{r0} \ll B_0$ so $n_t \approx n_0$, but with B_0 60-80 gauss, this is not so, It is found (2)(3)(4) that $\frac{\Delta n}{n_0} = \frac{n_t - n_0}{n_0}$ is positive and of the order of a few percent for both F and D magnets.

Some laboratories find also an $n' = -\frac{dn}{dr}$ at low fields. This effect is small ($n'/n \sim -0.3\%$ per cm), and depends very much on the

details of the magnet design.

A difference in B_{ro} is expected between F and D magnets (2)(5), while a small random fluctuation in the mean value of B_{to} for each magnet is reported by DESY (5). This fluctuation is due to variations in both B_{ro} and the vertical component of the stray field between magnets.

Pole face windings are provided to correct all these errors in the magnetic field of the NINA magnets.

1.2. Other Field Modifications.

In a synchrotron in which n is constant across the median plane, the number of betatron oscillations per revolution (Q) varies with particle momentum. This leads to a coupling of the betatron and synchrotron oscillations (6) which is undesirable. The variation in Q can be eliminated at injection by application of an n' to the fields of the F and D magnets by means of pole face windings. It should be noted however that under these conditions, Q is a function of betatron amplitude.

The windings producing n' alter B_{to} , the effect being different in the F and D magnets. This difference must be compensated.

1.3. Provision of Pole Face Windings.

Sets of windings producing separately the following magnetic fields are to be provided.

- (a) A dipole field (ie $\Delta B = \text{constant}$ across the magnet gap), variable independently in each magnet.
- (b) A dipole field the same in all F magnets and in all D magnets.
- (c) A quadrupole field, (ie $\Delta n = \text{constant}$, $\Delta B = 0$ at the equilibrium orbit), the field being the same in all F magnets and in all D magnets.
- (d) A sextupole field (ie $n' = \text{constant}$, $\Delta n = 0$ at the equilibrium orbit), again the field being the same in all F magnets and in all D magnets.

1.4. Outline of Design Method.

Following the method used in the design of the DESY pole face windings (5) the positions of the conductors are calculated first for hyperbolic pole faces. The corresponding conductor positions on the actual (non-hyperbolic) pole faces are determined from these.

It is not difficult to calculate the form of a continuous current distribution flowing on a pair of hyperbolic pole faces $\pm xy = \text{const.}$, and extending from $(x = 0, y = \pm \infty)$ to $(x = \pm \infty, y = 0)$, that will produce a quadrupole or a sextupole field. This current distribution is then replaced by a set of conductors all carrying the same current and spaced in such a way to approximate to the continuous current distribution. This approximation leads to fluctuations of the magnetic field about the required value, the closer the spacing of the wires, the smaller the fluctuations.

A further deviation from the ideal field distribution is caused by the termination of the sets of conductors approximately 6 cms on either side of the centre of the pole face profile. This deviation can be compensated by moving the outermost wires inwards.

The return conductors for the windings are located sufficiently far away from the pole faces to give negligible contribution to the magnetic field in the working region of the median plane. These conductors are so positioned that the E.M.F. induced in the windings by the main magnetic field is zero (section 7).

This cannot be done in the case of the dipole windings as these consist of conductors which link the whole of the main flux apart from a portion of the fringing flux. In this case a different method must be used to cancel the induced E.M.F.

1.5. Maximum Permissible Fluctuations.

These depend on the magnitude of the pole face winding field in use, that is, on $\Delta n/n_0$ (Quadrupole) and n' (Sextupole).

The windings have been designed to allow a maximum total fluctuation in their field index of $\pm 1/3\%$ of n_0 over the whole working region of the median plane, when the sextupole windings are providing the correct mean n' and the quadrupole windings are providing a mean $\Delta n/n_0 = 2\%$ in the F magnets and 1% in the D magnets.

2. The Continuous Current Distributions.

2.1. General Expression.

A pair of hyperbolic pole faces $xy = \pm \text{const} = \pm x_0 y_0$, is considered. The magnet poles are assumed to have infinite permeability. The equilibrium orbit is at the point $(x_0, 0)$.

A current ΔJ flows along the pole faces at right angles to the plane of the diagram (Fig.2) and in the same direction on both faces.

From Maxwell's Fourth Equation,

$$\oint \underline{H} \cdot d\underline{s} = \Delta J,$$

for a line integral around a closed path in the x-y plane which encloses the current. The path chosen is indicated in Fig.2. The contribution from that section of the path that is inside the magnet is zero as the iron is of infinite permeability. As Δt tends to zero the above expression becomes

$$\int_{\Delta s} H_t(s) ds = \Delta J$$

where $H_t(s) =$ tangential component of \underline{H}

thus $H_t(s) = dJ(s)/ds$

The calculation of $B_t(s) = \mu_0 H_t(s)$ is performed in the complex z - plane.

The unit vector along the contour is

$$\underline{z} / \sqrt{z \bar{z}},$$

$$\text{so } B_t = \mu_0 \frac{dJ}{ds} = \text{Re} \left\{ \bar{B} \frac{\bar{z}}{\sqrt{z\bar{z}}} \right\}$$

Multiplying both sides by

$$\sqrt{z\bar{z}}/x = ds/dx,$$

$$\mu_0 \frac{dJ}{dx} = \text{Re} \left\{ \bar{B} \frac{\bar{z}}{x} \right\} = \text{Re} \left\{ B \frac{z}{x} \right\} \quad (2)$$

In the present case it is necessary to find the forms of dJ/dx that will provide a quadrupole and a sextupole field.

2.2. Quadrupole Field.

The quadrupole field B_4 is added to the main field B . By analogy with equation (1), replacing dB/dx by dB_4/dx and bearing in mind that $B_{40}=0$,

$$n_t = n_0 + \frac{r_0}{B_0} \cdot \frac{dB_4}{dx} = n_0 + n_4$$

$$\text{i.e. } \Delta n = n_t - n_0 = \frac{r_0}{B_0} \frac{dB_4}{dx} = \text{constant for a quadrupole field.}$$

But for the main field,

$$n_0 = r_0/x_0, \text{ so}$$

$$\Delta n = x n_0 / B_0 \cdot dB_4/dx$$

Now for a quadrupole field,

$$B_y = K_1 x + K_2$$

$$B_x = K_1 y + K_3$$

But on the median plane, $B_x = 0$,

$$\text{and } B_y = 0 \text{ at } x = x_0,$$

$$\text{i.e. } B_x = K_1 y$$

$$B_y = K_1 (x - x_0)$$

Comparison with the expression for Δn shows that

$$K_1 = B_0 \Delta n / x_0 n_0$$

$$\text{so } B_4 = B_x + i B_y = i B_0 / n_0 \cdot \Delta n \cdot (\bar{z} - x_0) / x_0$$

Substitution into equation (2) gives

$$dJ/dx = B_0 y_0 / \mu_0 \cdot \Delta n / n_0 \cdot y / x$$

$$\text{or } dJ/dy = B_0 y_0 / \mu_0 \cdot \Delta n / n_0 = \text{constant} \quad (3)$$

2.3. Sextupole Field.

In this case $dn/dx = \text{constant} = n'$

while $\Delta n = 0$ at $x = x_0$

$$\text{i.e. } \Delta n(x) = n' (x - x_0)$$

The sextupole field is

$$B_6 = i B_0 \cdot n' / n_0 \cdot (\bar{z} - x_0)^2 / 2 x_0$$

Substitution into equation (2) gives

$$dJ/dx = B_0 y_0 / \mu_0 \cdot n' / n_0 \cdot (\bar{z} \bar{z} - x_0^2) / 2 x_0^2 \quad (4)$$

3. Calculation of the Conductor Positions.

3.1. Quadrupole Windings.

Each wire of the set is to carry the same current ΔJ ,

$$\text{where } \Delta J = \int_{x_1}^{x_2} dJ/dx \cdot dx = \int_{x_1}^{x_3} dJ/dx \cdot dx = \dots$$

$$\text{or } \Delta J = \int_{y_1}^{y_2} dJ/dy \cdot dy = \int_{y_1}^{y_3} dJ/dy \cdot dy = \dots \quad (5)$$

The wires will be situated at points somewhere between x_1 and x_2 , x_2 and x_3 , etc., but there is no unique point at which each wire can be placed in order to give exactly the correct magnetic field at all points in the median plane. A satisfactory field distribution is obtained if the wires are located at

$$y_w = \frac{y_1+y_2}{2}, \frac{y_2+y_3}{2}, \quad \text{etc.}$$

$$\text{where } x_1 y_1 = x_2 y_2 = \dots = x_w y_w.$$

For the quadrupole windings, equations (3) and (5) give

$$\Delta J_4 = \frac{B_0}{\mu_0} \cdot \frac{\Delta \eta}{n_0} \cdot \Delta y \quad (6)$$

i.e. the wires, each carrying current ΔJ , are equally spaced in the y - direction.

3.2. Sextupole Windings.

Equation (4) indicates that the direction of the current in the sextupole windings changes sign at a point near the equilibrium orbit position. At this point, dJ/dx is zero,

$$\text{i.e. } (z\bar{z} - x_0^2)/x^2 = 0,$$

$$\text{or } (x^2 + y^2 - x_0^2)/x^2 = 0,$$

$$\text{and as } xy = x_0 y_0 \quad \text{for points on the pole face,}$$

$$x^4 - x_0 x^2 + x_0^2 y_0^2 = 0.$$

The relevant solution is

$$x_c = \frac{x_0}{\sqrt{2}} [1 + \sqrt{1 - 4y_0^2/x_0^2}]^{1/2}$$

(Since $y_0 \sim x_0/10$, $x_c \sim x_0$).

Equation (5) now becomes

$$\Delta J = \int_{x_c}^{x_1} = \int_{x_1}^{x_2} = \dots \quad \text{and}$$

$$-\Delta J = \int_{x_{-1}}^{x_c} = \int_{x_{-2}}^{x_{-1}} = \dots,$$

where x_1 and x_{-1} are the points adjacent to x_c ;

Substitution for dJ/dx from equation (4) and integrating gives

$$\left[\frac{n_0 \mu_0}{h' B_0} \frac{1}{y_0} \right] \Delta J_0 = \left[\frac{x_1}{2} + \frac{x_0^2}{2x_1} - \frac{x_0^2 y_0^2}{6x_1^3} \right] - \left[\frac{x_c}{2} + \frac{x_0^2}{2x_c} - \frac{x_0^2 y_0^2}{6x_c^3} \right] = C - D \quad \left. \begin{array}{l} \\ \\ \end{array} \right\} - (7)$$

$$= \left[\frac{x_2}{2} + \frac{x_0^2}{2x_2} - \frac{x_0^2 y_0^2}{6x_2^3} \right] - \left[\frac{x_1}{2} + \frac{x_0^2}{2x_1} - \frac{x_0^2 y_0^2}{6x_1^3} \right] = \dots$$

$$\text{hence } \frac{x_2}{2} + \frac{x_0^2}{2x_2} - \frac{x_0^2 y_0^2}{6x_2^3} = 2C - D$$

$$\text{and in general } \frac{x_m}{2} + \frac{x_0^2}{2x_m} - \frac{x_0^2 y_0^2}{6x_m^3} = mC - (m-1)D \quad (8)$$

These equations can be solved for the x_m , while from equation (7) it can be seen that the magnitude of ΔJ is determined by the value of x_1 .

Two methods of location were tried for the conductors. These were :

$$x_w = \frac{x_c + x_1}{2}, \frac{x_1 + x_2}{2}, \text{ etc} \quad (9)$$

$$\text{and } x_w = \frac{1}{\Delta J_0} \int_{x_c}^{x_1} x \frac{dJ}{dx} dx, \text{ etc}$$

$$\text{i.e. } x_w = \frac{1}{2(C-D)} \left\{ \left[\frac{x_{m+1}^2}{2} - \frac{x_0^2 y_0^2}{2x_{m+1}^3} - x_0^2 \ln x_{m+1} \right] - \left[x_m \text{ term} \right] \right\} \quad (10)$$

Equation (10) was found to give the better results.

It is now necessary to develop a method by which the magnetic field produced by the set of wires at points (x_w, y_w) can be calculated.

4. Calculation of the Conductor Field Distribution.

4.1. Introduction.

The magnetic field distribution due to current carrying conductors on all four hyperbolic pole faces $xy = \pm y_0 y_0$ is calculated. This distribution can be used in the present case as the effect of the currents situated at points with negative x will have negligible effect in the positive x region under consideration.

In section 6 the treatment is extended to non-hyperbolic pole faces in order to provide a check on the present calculation.

4.2. Method of Calculation.

Maxwell's second and fourth equations can be expressed in the present case as

$$\oint (B_x dy - B_y dx) = 0 \quad (11)$$

and

$$\oint (B_x dx + B_y dy) = 0 \text{ or } \mu_0 \Delta J \quad (12)$$

The zero of equation (12) occurs if the path of integration in the plane $z = x+iy$ does not enclose the current ΔJ .

The magnetic field $B_x + i B_y$ must satisfy equations (11) and (12). Since it also satisfies Laplace's equation, it can be obtained from the analytic function.

$$\begin{aligned} F(x,y) &= U(x,y) + i V(x,y) \\ \text{where } V(x,y) &= \text{const. is a magnetic equi-potential,} \\ \text{and } U(x,y) &= \text{const. is a line of force.} \end{aligned}$$

Both U and V are real and U is a measure of the magnetic flux per unit length. The two functions are conjugate functions obeying the Cauchy - Riemann equations.

$$\partial u / \partial x = \partial v / \partial y, \quad \partial u / \partial y = - \partial v / \partial x.$$

The magnetic field is given by

$$\left. \begin{aligned} B_x + i B_y &= - \partial v / \partial x - i \partial v / \partial y \\ &= + \partial u / \partial y - i \partial u / \partial x \end{aligned} \right\} \quad (13)$$

Using equation (13), equations (11) and (12) can be combined in the form

$$\oint_{\gamma} \frac{dF}{dz} dz = \oint_{\gamma} F'(z) dz = 0 \text{ or } - i \mu_0 \Delta J \quad (14)$$

Thus the function must have a singularity at the current point

$$z_w = x_w + i y_w \quad \text{with residue } \frac{\mu_0 \Delta J}{2\pi}.$$

Because the pole faces are assumed to have infinite permeability, the lines $xy = \pm x_0 y_0$ must be equipotentials. The lines $x = 0$ and $y = 0$ are equipotentials for reasons of symmetry.

$$\text{Thus } V(x,y) = \text{Im. } (F) = \text{const. on } x = 0, y = 0, \text{ and } xy = \pm x_0 y_0. \quad (15)$$

Three conformal transformations are now applied to the region $x, y \geq 0$.⁽⁷⁾

(i) The z - plane, Fig. 3 (i) is transformed to the w - plane using the transformation.

$$w = z^2 / 2x_0 \quad (16a)$$

The pole face now becomes the straight line $v = y_0$ (Fig. 3) (ii), while $x = 0$, and $y = 0$ become $v = 0$.

(ii) The w - plane is transformed to the ζ - plane using the Schwarz - Cristoffel transformation

$$\frac{dw}{d\zeta} = \frac{y_0}{\phi_0} \cdot \frac{1}{\zeta} \quad (16b)$$

$v = 0$ becoming $\eta = 0$, $\zeta = 0$, while $u = y_0$ transforms to $\zeta = p e^{i\phi}$
(Fig. 3) (iii)

(iii) Finally the ζ - plane is transformed to the upper λ plane:

$$\lambda = \zeta^{\pi/\phi_0} \quad (16c)$$

the pole face becoming $\gamma = 0$, $\sigma \leq 0$.

Corresponding to $F(z)$ in the z plane there is an analytic function $G(\lambda)$ in the λ - plane.

Equation (15) is now replaced by

$$\text{Im}(G) = \text{const} (=0) \text{ on the real } \lambda\text{-axis}, \quad (17)$$

while

$$\oint_{\lambda} G'(\lambda) d\lambda = \oint_z \frac{dG}{dz} \frac{dz}{d\lambda} d\lambda = \oint_z F'(z) dz = 0 \text{ or } -i\mu_0 \Delta J \quad (18a)$$

The function $G(\lambda)$ will be a function of the co-ordinates of the current point $\lambda_w = \sigma_w$, $\sigma_w \leq 0$, while the path of the integral in the λ - plane must remain in the region $\gamma \geq 0$. Because of this restriction, λ_w is replaced by two points $\lambda_w = \sigma_w + i\delta\tau_w$, (which is within the region of integration), and $\sigma_w - i\delta\tau_w$ (which is not), and $\delta\tau_w$ can be made to approach zero.

Equation (18a) can now be expressed as follows:-

$$G'(\lambda) \text{ has a singularity at point } \lambda_w \text{ with residue } \mu_0 \Delta J / 2\pi \quad (18b)$$

$$\text{Now } B_x - iB_y = \partial u / \partial y + i \partial v / \partial y$$

$$= i \frac{dF}{dz}$$

$$= i \frac{dG}{d\lambda} \cdot \frac{d\lambda}{dz} \quad (19)$$

and we require that for both quadrupole and sextupole fields,

$$B = B_x + iB_y = 0 \text{ at } x = x_0.$$

It can be seen that equations (19) are satisfied by the function

$$G(\lambda) = \frac{\mu_0 \Delta J}{2\pi} \left[\ln(\lambda - \lambda_w)(\lambda - \lambda_w^*) - (\ln \lambda) \left(\frac{\lambda_0}{\lambda_0 - \lambda_w} + \frac{\lambda_0}{\lambda_0 - \lambda_w^*} \right) \right]$$

for which $G'(\lambda) = \frac{\mu_0 \Delta J}{2\pi} \left[\frac{1}{\lambda - \lambda_w} + \frac{1}{\lambda - \lambda_w^*} - \frac{1}{\lambda} \left(\frac{\lambda_0}{\lambda_0 - \lambda_w} + \frac{\lambda_0}{\lambda_0 - \lambda_w^*} \right) \right]$ (20)

As $\delta\tau_w \rightarrow 0$, $\lambda_w \rightarrow \lambda_w^*$, i.e. λ_w becomes real, so condition (17) is satisfied,

while $G'(\lambda) = 0$ for $\lambda = \lambda_0$ so from equation (19) it can be seen that $B_x = B_y = 0$ at $x = x_0$ unless $\frac{d\lambda}{dz} = \infty$ at $\lambda = \lambda_0$. This is not so.

Now $d\lambda/dz = \frac{d\lambda}{dz} \frac{dz}{dw} \frac{dw}{dz} = \frac{\pi z \lambda}{x_0 y_0}$, from equations (16)

Thus $B_x - iB_y = i \frac{\mu_0 \Delta J}{2\pi} \left[\frac{1}{\lambda - \lambda_w} - \frac{2\lambda_0}{\lambda_0 - \lambda_w} \right] \frac{\pi z}{x_0 y_0}$ from (19) and (20) (21)

We can express λ in terms of z by means of equations (16)

Thus $w = \frac{z^2}{2x_0} = \frac{y_0}{\phi_0} \ln \zeta = \frac{y_0}{\pi} \ln \lambda$

i.e. $\lambda = \exp \frac{\pi}{2} \left[\frac{z^2}{x_0 y_0} \right] = \exp \frac{\pi}{2} \left[\frac{x^2 - y^2 + 2ixy}{2x_0 y_0} \right]$.

For points λ_w , $xy = x_0 y_0$, and

$$\lambda_w = \exp \frac{\pi}{2} \left[\frac{x_w^2}{x_0 y_0} - \frac{x_0 y_0}{x_w^2} \right] \exp[i\pi]$$

i.e. $\lambda_w = -\exp \frac{\pi}{2} \left[\frac{x_w^2}{x_0 y_0} - \frac{x_0 y_0}{x_w^2} \right]$ (22a)

For points on the median plane, $y = 0$, so

$$\lambda = \exp \frac{\pi}{2} \left[\frac{x^2}{x_0 y_0} \right]$$
 (22b)

while for $(x, y) = (x_0, 0)$,

$$\lambda_0 = \exp \frac{\pi}{2} \left[\frac{x_0}{y_0} \right]$$
 (22c)

Using equations (22), the field at a point $(x, 0)$ on the median plane is, from (21)

$$\begin{aligned} B_x &= 0 \\ B_y &= \frac{\mu_0 \Delta J}{x_0 y_0} \cdot x \cdot \left[\frac{1}{1+E} - \frac{1}{1+E_0} \right] \end{aligned}$$
 (23)

where $E = \exp \frac{\pi}{2} \left[\frac{x_w^2}{x_0 y_0} - \frac{x_0 y_0}{x_w^2} - \frac{x^2}{x_0 y_0} \right]$

and $E_0 = \exp \frac{\pi}{2} \left[\frac{x_w^2}{x_0 y_0} - \frac{x_0 y_0}{x_w^2} - \frac{x_0}{y_0} \right]$

The contribution Δn to the field index is

$$\Delta n(x) = \frac{\tau_0}{B_0} \frac{dB_y}{dx} = \frac{\mu_0 \Delta J \tau_0}{B_0 y_0} \cdot A_w$$
 (24)

with $A_w = \frac{1}{1+E} \left[1 + \frac{\pi x^2}{x_0 y_0} \cdot \frac{E}{1+E} \right] - \frac{1}{1+E_0}$

Equations (23) and (24) refer to a single conductor at point (x_w, y_w) carrying current J . For a set of conductors, the expressions must be summed over the co-ordinates x_w of all the wires.

5. Comparison of Ideal and Real Fields.

5.1. The Quadrupole Fields.

In section 3.1 it was shown that the quadrupole wire positions are

$$y_w = \pm (y_c \pm m \Delta y)$$

$$x_w = x_{oy} / y_w$$

where y_c is arbitrary and m is an integer.

The contribution $\Delta n(x)$ from wires in these positions is, from equation (24)

$$\Delta n(x) = \frac{\mu_0 \Delta J n_0}{B_0 y_0} \sum_w A_w$$

while the ideal contribution is, from equation (6) section 3.1,

$$\Delta n_i = \frac{\mu_0 \Delta J n_0}{B_0 \Delta y}$$

$$\text{since } (dJ/dy)_4 = \Delta J / \Delta y$$

$$\text{Thus } \Delta n(x) / \Delta n_i = \frac{\Delta y}{y_0} \sum_w A_w \quad (25)$$

It is necessary to choose Δy sufficiently small to keep fluctuations in this quantity within tolerance over the working region of the median plane. When necessary, the outermost wires are moved inwards (section 1.4)

5.2. The Sextupole Fields.

In this case the conductor positions are given by equations (9) and (10) of section 3.2, and

$$\Delta n(x) = \frac{\mu_0 \Delta J n_0}{B_0 y_0} \sum_w \pm A_w,$$

the positive sign being taken if $x_w > x_c$ (section 3.2).

The ideal contribution to the field index is, from section 2.3,

$$\Delta n_i(x) = n'(x - x_0),$$

while from equation (7) section 3.2,

$$n' = \frac{\mu_0 \Delta J n_0}{B_0 y_0} \cdot \frac{1}{C-D}$$

$$\text{i.e. } n_i(x) = \frac{\mu_0 \Delta J n_0}{B_0 y_0} \cdot \frac{x - x_0}{C-D}.$$

To compare the real and ideal contributions at point x , we calculate

$$\frac{[\Delta n(x) - \Delta n_i(x)]}{\Delta n_i(x = x_0 + 1 \text{ cm})} = (C-D) \sum_w \pm A_w - (x - x_0) \quad (26)$$

The outermost wires are once more moved inwards.

6. Non-Hyperbolic Pole Faces.

6.1. Introduction.

Hyperbolic pole faces, which supply a quadrupole field, extend from $x = 0, y = \pm \infty$ to $x = \infty, y = 0$. The NINA pole faces ⁽¹⁾ illustrated in Fig. 4, are not hyperbolic, being so shaped that with a total width of 23 cms. (F) and 21.5 cms (D), the field index n is within $\pm 1\%$ of the correct value over 13 cms (F) and 9 cms (D) of the median plane.

6.2. Position of the Pole Face Windings.

The conformal transformations of section 4.2 can be modified for use with the non-hyperbolic pole faces. It is possible by using these to find the co-ordinates of the current points on the non-hyperbolic contour corresponding to those on the hyperbolic contour and giving the same field distribution in the median plane.

For the non-hyperbolic pole faces, equation (16b) becomes

$$dw/dz = y_0/\phi_0 \cdot 1/z \cdot \beta(z) \quad (27)$$

$$\text{with } \beta(z) = (1+z)^{2-\omega/\pi} / (1+\alpha/2)(1+z/\gamma) \quad (28)$$

where α, γ and ω are constants.

Equations (19) and (20) of section 4.2 remain unaltered, while

$$d\lambda/dz = \pi/x_0 y_0 \cdot \lambda \cdot z \cdot \beta(z)$$

Equation (21) becomes

$$B_x - iB_y = i \frac{\mu_0}{x_0 y_0} \Delta J \cdot \beta(z) z \left[\frac{\lambda}{\lambda - \lambda_w} - \frac{\lambda_0}{\lambda - \lambda_w} \right] \quad (29)$$

It should be noted that B, z and λ refer to the point at which the field is being calculated.

In the present case, we are considering the magnetic field distribution at points in the median plane not far removed from the equilibrium orbit. At the values of x and z corresponding to these points, $\beta = 1$ to a good approximation. Thus all factors outside the square bracket of equation (29) are the same as those of equation (21). Inside the bracket, λ_0 and λ are the same in both cases if $\beta = 1$, as transformations (16b) and (27) are then identical. If the fields are to be the same, corresponding values of λ_w must be the same. Since λ, λ_0 and λ_w are equal for the current points on the hyperbolic and non-hyperbolic contours, then

$$G(\lambda) = \frac{\mu_0 \Delta J}{\pi} \left[\ln(\lambda - \lambda_w) - \frac{\lambda_0}{\lambda_0 - \lambda_w} \ln \lambda \right]$$

must be also, as must $\operatorname{Re} G(\lambda)$

Now $\operatorname{Re} G(\lambda)$ is the magnetic flux per unit length, so the field distributions will be identical for the hyperbolic and non-hyperbolic pole faces, (subject to the approximation that $\beta = 1$), if the conductors are situated at points

on the contours having equal values of flux per unit length.

By reason for the conformal properties of the transformations, this must also be true in the z - plane. For a quadrupole field and a hyperbolic pole face,

$$U = (x_w^2 - y_w^2) / 2x_0 \quad \text{--- (30)}$$

while the value of U , for a quadrupole, at any point on the non-hyperbolic pole face can be calculated ⁽¹⁾. Since the two U values differ by a constant, it is necessary to equate differences in U between the current point and an arbitrary point, (x_0, y_0) for example. These differences represent the total flux enclosed.

Since x_w is known for each current point on the hyperbolic pole face, the above method can be used to calculate the corresponding points on the non-hyperbolic pole face.

6.3. Calculation of the P.F.W. Field Distribution.

The values of z corresponding to points (x_w, y_w) , $(x, 0)$ and $x_0, 0$ for the non-hyperbolic pole faces are known ⁽¹⁾. From these, λ_w , λ and λ_0 are obtained from the transformation equation (16c), and the magnetic field at $(x, 0)$ due to a current flowing at (x_w, y_w) can be calculated using equations (28) and (29). Since this procedure does not involve the approximation $\beta = 1$, it can be used to estimate the errors incurred by this approximation in the method used to locate the conductors on the non-hyperbolic pole face.

On the median plane, equation (29) takes the form

$$\left. \begin{aligned} B_y &= \frac{\mu_0}{x_0 y_0} \Delta J \beta x \left[\frac{1}{1 - \lambda_w / \lambda} - \frac{1}{1 - \lambda_w / \lambda_0} \right] \\ \text{and } \frac{\partial B_y}{\partial x} &= \frac{\mu_0}{x_0 y_0} \Delta J \frac{\partial}{\partial x} \left\{ \beta x \left[\frac{1}{1 - \lambda_w / \lambda} - \frac{1}{1 - \lambda_w / \lambda_0} \right] \right\} \end{aligned} \right\} \quad \text{--- (31)}$$

From the transformation equations (16a) (16c) and (27),

$$\begin{aligned} \frac{\partial z}{\partial x} &= \frac{\phi_0}{x_0 y_0} \cdot z \cdot \beta \cdot x \\ \text{and } \frac{\partial \lambda}{\partial x} &= \frac{\pi}{x_0 y_0} \cdot \lambda \cdot \beta \cdot x \end{aligned}$$

From equation (28),

$$\frac{\partial \beta}{\partial z} = \beta \left[\frac{2 - \omega \pi}{1 + z} - \frac{1}{\alpha + z} - \frac{1}{\gamma + z} \right]$$

Using these together with equation (31),

$$\frac{\partial B_y}{\partial x} = \frac{\mu_0 \Delta J}{x_0 y_0} \cdot \beta \cdot B_w, \text{ where}$$

$$B_w = \left\{ \left(\frac{1}{1 - \lambda_w / \lambda} - \frac{1}{1 - \lambda_w / \lambda_0} \right) \left[1 + \frac{\phi_0}{x_0 y_0} \cdot z \cdot \beta x \left(\frac{2 - \omega \pi}{1 + z} - \frac{1}{\alpha + z} - \frac{1}{\gamma + z} \right) \right] - \frac{\pi x^2 \beta \lambda_w}{x_0 y_0 \lambda (1 - \lambda_w / \lambda)^2} \right\}$$

$$\text{Also } \Delta n(x) = \Delta n_d = \frac{\tau_0}{B_0} \frac{\partial B_y}{\partial x}, \quad \text{and } n_0 = \frac{r_0}{x_0}$$

$$\text{so } \frac{\Delta n_d}{n_0} = \frac{\mu_0}{B_0} \frac{\Delta J}{y_0} \beta B_w$$

This can be compared with equation (24), section 4.2. containing the values x'_w for the current points on the hyperbolic profile :

$$\Delta n_d - \Delta n = \frac{\mu_0}{B_0} \frac{\Delta J}{y_0} \left[\beta B_w - A_w \right] \quad \text{--- (32)}$$

7. Induced E.M.F. and Forces.

7.1. Induced E.M.F.

The pole face windings and their wires form closed loops linking the flux of the main magnetic field. Since this flux is changing with time, an E.M.F. is induced.

In Fig. 5(a) the magnetic field is normal to the plane of the paper. If the field strength B is assumed independent of z , while $\frac{dB}{dt}$ is independent of both x and z ,

$$B(x, z, t) = B(x) f(t),$$

$$\text{and } E = -\frac{\partial \phi}{\partial t} = -\frac{\partial}{\partial t} \int_{z_1}^{z_2} \int_{x_1}^{x_2} B(x, z, t) dx dz$$

$$= (z_2 - z_1) \frac{df}{dt} \int_{x_1}^{x_2} B(x) dx$$

$$\text{but } \int_{x_1}^{x_2} B(x) dx = U(x_2) - U(x_1) \quad \text{From section 4.2, so}$$

$$E = (z_2 - z_1) \frac{df}{dt} [U(x_2) - U(x_1)].$$

Since the pole faces of the magnets are not in the (x, z) plane, the magnetic field at the contour is no longer perpendicular to this plane and the expression for E becomes

$$E = (z_2 - z_1) \frac{df}{dt} [U(x_1, y_1) - U(x_2, y_2)] \quad (33)$$

Fig. 5(b) shows a simple two wire quadrupole winding. The dotted line indicates the position of the equilibrium orbit while the arrows show the direction of flow of the exciting current. Wires 3 and 4 are the return conductors. These are placed on the pole face at positions sufficiently remote from the equilibrium orbit that they give negligible contribution to the field index in the working region of the median plane. The relative positions of these conductors are determined such that the total induced E.M.F. is zero. If $(z_1 - z_2)$ is assumed to be the same for all the conductors, equation (33) shows that for $E = 0$,

$$(U_3 - U_1) - (U_2 - U_4) = 0$$

$$\text{i.e. } U_1 + U_2 = U_3 + U_4 \quad (34)$$

A two wire sextupole winding is illustrated in Fig. 5(c). Return wires are not necessary in this case, the two outer conductors constituting a dipole winding in series with the sextupole. This is necessary in order to reduce the induced E.M.F. to zero. For these wires E is zero if

$$U_1 - U_2 = U_3 - U_4 \quad (35)$$

This method of determination of the outer wire positions involves the following approximations.

(a) Because of the small angle between the blocks of which the magnets are constructed, $(z_1 - z_2)$ is not constant, varying by about 0.2 cms. across the magnet profile. Since the wires have a length 330 cms, this effect is expected to be very small.

(b) The magnetic field distribution is modified by the presence of the gaps between blocks.

(c) The ends of the magnets are terminated by end blocks which are so designed that the 'B - length' of the magnet is independent of x. The conductors do not follow the profile of the end blocks but for several centimetres they continue in their original straight line into the region between the poles of the end block where they are connected by cross wires $z = \text{constant}$. These cross wires are situated in a region where the magnetic field is reduced below its full value. The fractional reduction both at the end blocks and in the gaps between blocks is a function of x.

7.2. Forces on the Conductors.

The pole face windings are current carrying conductors situated in the main magnetic field B . The force on each conductor of length l metres and carrying current i amps will be

$$\underline{F} = i \underline{l} \wedge \underline{B} \quad (36)$$

This force will be in the x - y plane and tangential to the pole face. As B varies with position on the pole face, the forces on the wires will not in general be equal in magnitude. They are largest at peak field.

Forces also arise from the influence of currents i_1 and i_2 in neighbouring conductors. In this case

$$\underline{F} = \frac{\mu_0 i_1 i_2}{2\pi r} \underline{l} \wedge \underline{r} \quad (37)$$

where \underline{r} is the vector joining the two wires.

8. The Sextupole Field.

8.1. Calculation of n'

As explained in Section 1.2, it is desirable to reduce the variation in the number of betatron oscillations per revolution (Q) with variations in particle momentum. It is possible to do this simultaneously for vertical and horizontal oscillations by addition to the main magnetic field a constant $n' = \frac{dn}{dx}$ the magnitude of n' differing in the F and D magnets. The method used is described in a CEA paper ⁽⁶⁾, so it is proposed to give only a short summary of the method.

Neglecting second order terms, the equations of motion for the horizontal and vertical betatron oscillations about the equilibrium orbit are, respectively,

$$\begin{aligned} \frac{d^2 x}{d\ell^2} + \left(\frac{1}{B_e r_e} \frac{dB}{dx} \right) x &= 0 \\ \frac{d^2 y}{d\ell^2} + \left(\frac{1}{B_e r_e} \frac{dB}{dx} \right) y &= 0, \end{aligned}$$

where B_e and r_e are the magnetic field in the median plane and the magnetic radius corresponding to a particle of momentum p_e , and ℓ is a distance measured along the equilibrium orbit.

$\frac{dB}{dx}$ is evaluated at the point in the median plane where $r = r_e$

The equilibrium parameters are related by

$$p_e = B_e e r_e$$

where e = electric charge of the particle.

$$\text{Thus } d^2x/d\ell^2 + \left(\frac{e}{p_e} \frac{dB}{dx}\right) x = 0$$

$$\text{and } d^2y/d\ell^2 + \left(\frac{e}{p_e} \frac{dB}{dx}\right) y = 0.$$

It can be seen from these expressions, that if $\frac{dB}{dx}$ is independent of r_e , the restoring force is inversely proportional to the particle momentum.

If, however, d^2B/dx^2 is not zero,

$$\delta\left(\frac{1}{p_e} \frac{dB}{dx}\right) = \frac{1}{p_e} \left[\frac{d^2B}{dx^2} \frac{dx}{dp_e} - \frac{1}{p_e} \frac{dB}{dx} \right] \delta p_e.$$

The change in Q at a given azimuthal position with change δp_e in the momentum can be shown ⁽⁸⁾ to be proportional to

$$\left[\frac{d^2B}{dx^2} \frac{dx}{dp_e} - \frac{1}{p_e} \frac{dB}{dx} \right],$$

and to the magnitude of the amplitude function β_x or β_y .

$$\text{Putting } \alpha(\ell) = \frac{1}{r_0} p \frac{dz}{dp},$$

$$\delta Q_x(\ell) \propto \beta_x(\ell) \left[r_0 \alpha(\ell) \frac{d^2B}{dx^2} - \frac{dB}{dx} \right]$$

$$\text{and } \delta Q_y(\ell) \propto \beta_y(\ell) \left[r_0 \alpha(\ell) \frac{d^2B}{dx^2} - \frac{dB}{dx} \right].$$

Thus zero variation of Q with momentum is achieved if

$$\int \delta Q_x(\ell) d\ell = 0$$

$$\text{and } \int \delta Q_y(\ell) d\ell = 0,$$

where the integral is taken over one period FODO of the magnet structure. The only contribution to the integral in the straight sections O and \bar{O} is that of the fringing fields and stray fields. This contribution has not been included in the integral. Substituting for Q , and putting $B' = \frac{dB}{dx}$, $B'' = \frac{d^2B}{dx^2}$,

$$B_F'' \tau_0 \int_F \beta_x(l) \alpha(l) dl + B_D'' \tau_0 \int_D \beta_x(l) \alpha(l) dl = B_F' \int_F \beta_x(l) dl + B_D' \int_D \beta_x(l) dl$$

$$\text{and } B_F'' \tau_0 \int_F \beta_y(l) \alpha(l) dl + B_D'' \tau_0 \int_D \beta_y(l) \alpha(l) dl = B_F' \int_F \beta_y(l) dl + B_D' \int_D \beta_y(l) dl \quad (38)$$

Since $\alpha(l)$, $\beta(l)$, τ_0 , B' are all known⁽⁹⁾ these equations can be solved for B_F'' and B_D'' after performing the necessary numerical integrations.

Finally the values of n_F' and n_D' are obtained from

$$n' = \frac{r_0}{B_0} B''$$

9. Numerical Results.

9.1. Magnet parameters.

'D' Magnet:

x_0	=	44.033 cms.
y_0	=	3.810 cms.
n_0	=	47.169

'F' Magnet:

x_0	=	44.986 cms.
y_0	=	3.048 cms.
n_0	=	46.169

9.2. Hyperbolic Pole Faces.

In the following table the figures in brackets are the modified co-ordinates after the outermose wires have been shifted inwards. The field distributions provided by these windings both before and after this correction are illustrated in Figs. 6 - 11. The U - values correspond to the modified positions. Expressions (25), (26) and (24) have been used in the calculations. Suitable values of Δy (Quadrupole) and x_1 (Sextupole) were determined by trial-and-error.

'D' Magnet:

Δy	=	0.2875 cms.
x_1	=	48.000 cms.

Winding Type	Wire Number	x cms.	U
Quadrupole	Q1	37.096 (37.75)	+ 15.958
	Q2	39.614	+ 17.616
	Q3	42.499	+ 20.332
	Q4	45.838	+ 23.707
	Q5	49.745	+ 27.970
Total U=+105.583			
Sextupole	S1	37.102 (38.50)	+ 16.616
	S2	38.044 (38.75)	+ 16.838
	S3	39.282	+ 17.315
	S4	41.305	+ 19.186
	S5	46.592	- 24.503
	S6	48.938	-27.061
	S7	50.524 (50.30)	-28.603
Total U=-10.214			

'F' Magnet :

$$\Delta y = 0.1650 \text{ cms.}$$

$$x_1 = 48.000 \text{ cms.}$$

Winding Type	Wire Number	x cms.	U
Quadrupole	Q1	36.093 (37.05)	+15.105
	Q2	37.732 (37.75)	+15.692
	Q3	39.527	+17.231
	Q4	41.501	+19.022
	Q5	43.682	+21.098
	Q6	46.106	+23.528
	Q7	48.814	+26.396
	Q8	51.850	+29.803
			Total U = +167.875
Sextupole	S1	35.627 (36.30)	+14.488
	S2	36.505 (36.80)	+14.898
	S3	37.384	+15.385
	S4	38.428	+16.272
	S5	39.815	+17.488
	S6	42.054	+19.539
	S7	47.924	-25.435
	S8	50.850	-28.657
	S9	52.383 (52.10)	-30.093
			Total U = +13.889

9.3 Return Conductors & Dipoles.

These are positioned so as to satisfy equations (34) and (35).

'D' Magnet:

Winding Type	Wire Number	U
Quadrupole	Q6	-12.800)
	Q7	-13.050)
	Q8	-13.300)
	Q9	-33.016)
	Q10	-33.417)
		Total U -105.583
Sextupole	S8	+12.300)
	S9	+12.550)
	S10	-35.064)
		Total U = -10.214
Dipole	D1	+34.850)
	D1	-13.550)
		Total U = +21.300
Dipole	D2	+34.050)
		-13.800)
		Total U = +20.250.

'F' Magnet.

Winding Type	Wire Number	U	
Quadrupole	Q9	-11.400	
	Q10	-11.550	
	Q11	-11.700	
	Q12	-11.900	Total U = -167.875.
	Q13	-12.100	
	Q14	-36.150	
	Q15	-36.400	
	Q16	-36.675	
Sextupole	S10	-11.280	
	S11	-12.350	
	S12	-12.600	Total U = -13.889.
	S13	-12.850	
	S14	+35.191	
Dipole	D1	+34.400	
	D1	-13.100	Total U = +21.300.
Dipole	D2	+34.750	Total U = +23.590

9.4 Non-Hyperbolic Pole Faces.

The method described in section 6.2 was used to determine the positions of the wires on the non-hyperbolic pole faces. In the following tables the sense of the current in each conductor is given as well as the co-ordinates of the points on the pole faces at which the conductors are to be located. The wire positions are illustrated in figs. 12 and 13.

'D'MAGNET.

Winding Type	Wire Number	Current	x cms.	y cms.
Quadrupole	Q1	(+)	37.579	4.330
	Q2	(+)	39.604	4.267
	Q3	(+)	42.479	3.950
	Q4	(+)	45.837	3.660
	Q5	(+)	49.769	3.363
	Q6	(-)	35.433	5.105
	Q7	(-)	35.570	4.890
	Q8	(-)	35.692	4.700
	Q9	(-)	53.271	3.528
	Q10	(-)	53.467	3.713
Sextupole	S1	(+)	38.463	4.394.
	S2	(+)	38.687	4.382.
	S3	(+)	39.263	4.315
	S4	(+)	41.308	4.074
	S5	(-)	46.596	3.602
	S6	(-)	48.938	3.434
	S7	(-)	50.325	3.297
	S8	(-)	35.174	5.649
	S9	(-)	35.306	5.364
	S10	(+)	54.209	5.189
Dipole	D1	(-)	35.819	4.542
	D1	(+)	54.112	4.900
Dipole	D2	(-)	35.956	4.415
	D2	(+)	53.762	4.125

Winding Type	Wire Number	Current	x cms.	y cms.
Quadrupole	Q1	(+)	36.896	3.708
	Q2	(+)	37.724	3.680
	Q3	(+)	39.527	3.472
	Q4	(+)	41.498	3.302
	Q5	(+)	43.680	3.139
	Q6	(+)	46.104	2.974
	Q7	(+)	48.814	2.809
	Q8	(+)	51.854	2.647
	Q9	(-)	34.618	5.659
	Q10	(-)	34.681	5.375
	Q11	(-)	34.745	5.116
	Q12	(-)	34.828	4.811
	Q13	(-)	34.912	4.531
	Q14	(-)	55.900	3.838
	Q15	(-)	55.984	4.158
	Q16	(-)	56.068	4.587
Sextupole	S1	(+)	36.172	3.508
	S2	(+)	36.609	3.653
	S3	(+)	37.305	3.724
	S4	(+)	38.433	3.584
	S5	(+)	39.820	3.444
	S6	(+)	42.050	3.261
	S7	(-)	47.927	2.860
	S8	(-)	50.851	2.697
	S9	(-)	52.083	2.634
	S10	(-)	34.572	5.906
	S11	(-)	35.019	4.239
	S12	(-)	35.126	3.988
	S13	(-)	35.235	3.790
	S14	(+)	55.540	3.000
Dipole	D1	(+)	35.344	3.632
	D1	(-)	55.164	2.634
	D2	(+)	34.524	6.144
	D2	(-)	55.344	2.771

9.5 Direct Calculation of Field Index.

The method of section 6.3 has been used to calculate directly the field index provided by the conductors of the last section. The results are illustrated by the dotted curves in figures 6 to 11.

9.6 Forces On the Conductors.

The forces between two conductors have been calculated by means of equation 37, section 7.2. Taking $i_1 = 1$ Amp, $r = 2$ mms, $l = 3.26$ metres,

$$F = 0.033 \text{ gms. wt.}$$

Forces on the conductors due to the main magnetic field have been obtained using equation 36 with $i = 1$ Amp, $l = 3.26$ metres and magnetic fields that correspond to one of 6.43 kilo-Gauss at the equilibrium orbit. The corresponding magnetic field strengths at the conductor positions on the pole faces are known from the pole face contour calculations (1).

In the table that follows, the forces, which can be taken to be in a direction tangential to the magnet pole face profile and in the x - y plane, have been listed. The signs of the forces have been made to follow the current direction convention of section 9.4.

Winding Type	Wire No.	'D' Magnet force Gm.wt,	'F' Magnet force Gm.wt.
Quadrupole	Q1	+186	+148
	Q2	+188	+165
	Q3	+208	+188
	Q4	+223	+199
	Q5	+240	+208
	Q6	-197	+220
	Q7	-220	+233
	Q8	-244	+244
	Q9	-327	-107
	Q10	-297	-118
	Q11	-	-126
	Q12	-	-141
	Q13	-	-161
	Q14	-	-176
	Q15	-	-150
	Q16	-	-131

Winding Type	Wire Number	'D' Magnet Force Gm.Wt.	'F' Magnet Force Gm. Wt.
Sextupole	S1	+165	+227
	S2	+169	+163
	S3	+192	+148
	S4	+201	+182
	S5	-227	+191
	S6	-235	+201
	S7	-248	-229
	S8	-161	-242
	S9	-178	-244
	S10	+154	-101
	S11	-	-189
	S12	-	-212
	S13	-	-255
	S14	-	+189
Dipole	D1	-274	-300
	D1	+169	+338
Dipole	D2	-302	-96
	D2	+240	+343

Examination of Figs. 12 and 13 shows that the conductors can be divided into three groups such that the forces on all conductors of each group are approximately co-linear. These groups are as follows:-

$S_8 - D_2,$	$Q_1 - S_7$ and $Q_9 - S_{10},$	'D' Magnet.
$D_2 - D_1,$	$S_1 - S_9$ and $D_1 - Q_{16},$	'F' Magnet.

The forces in these groups have been added algebraically with the force directions of the table above. The results are given in Fig. 14. The second diagram in each case shows the resultant forces when the currents in the Sextupole and Dipole windings are reversed.

9.7 Magnitude of the Sextupole Fields.

Equations 38, section 8.1 have been used to calculate n' for the 'F' and 'D' magnets. The results are as follows:-

Magnet	n' (per cm).	n'/n_0 (% per cm).
D	+0.40978	+0.86875
F	-0.22975	+0.49763

9.8 Magnitude of Exciting currents.

These are evaluated by means of equations 6, and 7 of section 3 for quadrupole and sextupole windings. The main excitation current of the magnets in amps is $I = B_0/13.19$, B_0 being in Gauss, and for the dipole windings, $B_0 = 0.330 \Delta J$, (D), $0.412 \Delta J$, (F).

$$\text{Thus } \frac{\Delta B_0}{B_0} = \frac{\Delta J}{401} = \frac{.330 \Delta J}{B_0} \quad \text{for 'D' Magnets and}$$

$$\frac{\Delta B_0}{B_0} = \frac{\Delta J}{321} = \frac{.412 \Delta J}{B_0} \quad \text{for 'F' magnets.}$$

Taking $B_0 = 64.3$ Gauss leads to the following results, which may be taken to be typical operating parameters:

Magnet Winding	$\frac{\Delta B_0}{B_0}$ (%)	$\frac{\Delta n}{n_0}$ (%)	$\frac{n'}{n_0}$ (% per cm)	ΔJ (amps)
D Dipole	1.0	-	-	1.948
Quadrupole	-	1.0	-	0.147
Sextupole	-	-	0.869	0.300
F Dipole	1.0	-	-	1.560
Quadrupole	-	2.0	-	0.169
Sextupole	-	-	0.498	0.166

10. Excitation of the Windings.

The windings will be excited by D.C. currents of up to 2 amperes. The quadrupole conductors of each magnet type (F or D) will all be connected in series as will the sextupole conductors. The dipole windings of section 1.3 (b) have been arranged to enclose the same total flux in the F and D magnets (see section 9.3). The induced voltages in these windings will be balanced out if all conductors both F and D, are connected in series in the correct manner. The other type of dipole windings, section 1.3 (a), constitute a separate circuit on each magnet.

The conductor cross sections will be chosen to allow operation with a 100-200 volt power supply.

11. References.

- (1) V.W. Hatton and H.C. News, NIRS Electron Laboratory, EL/TM-4.
- (2) Deutsches Elektronen- Synchrotron DESY A 2.84.
- (3) R. Yamada and Y Kobayashi, Tokyo Institute for Nuclear Study, INSJ-28, TH-37.
- (4) E. Regenstreif, CERN 59-29
- (5) W. Hardt. Deutsches Elektronen - Synchrotron Laboratory, DESY A.19.
- (6) K.W. Robinson, Cambridge Electron Accelerator, CEA-62.
- (7) G. Rippen DESY A 2.77.
- (8) Sturrock, Annals of Physics, 3/1, 1958.
- (9) I.I. Rabonowitz, M.Sc. Thesis, University of Liverpool, 1962.

12. Acknowledgments.

I would like to thank Dr. W. Hardt on whose work this report is almost entirely based, Dr. H.C. News, and Mr. V.W. Hatton for all the help and advice they have given.

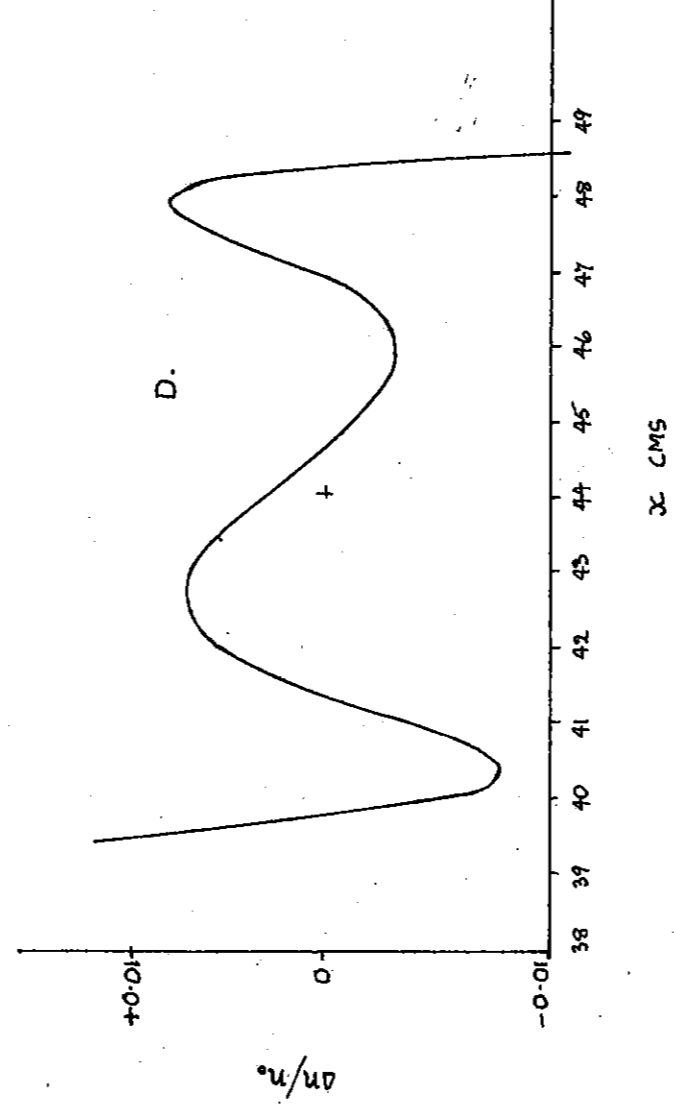
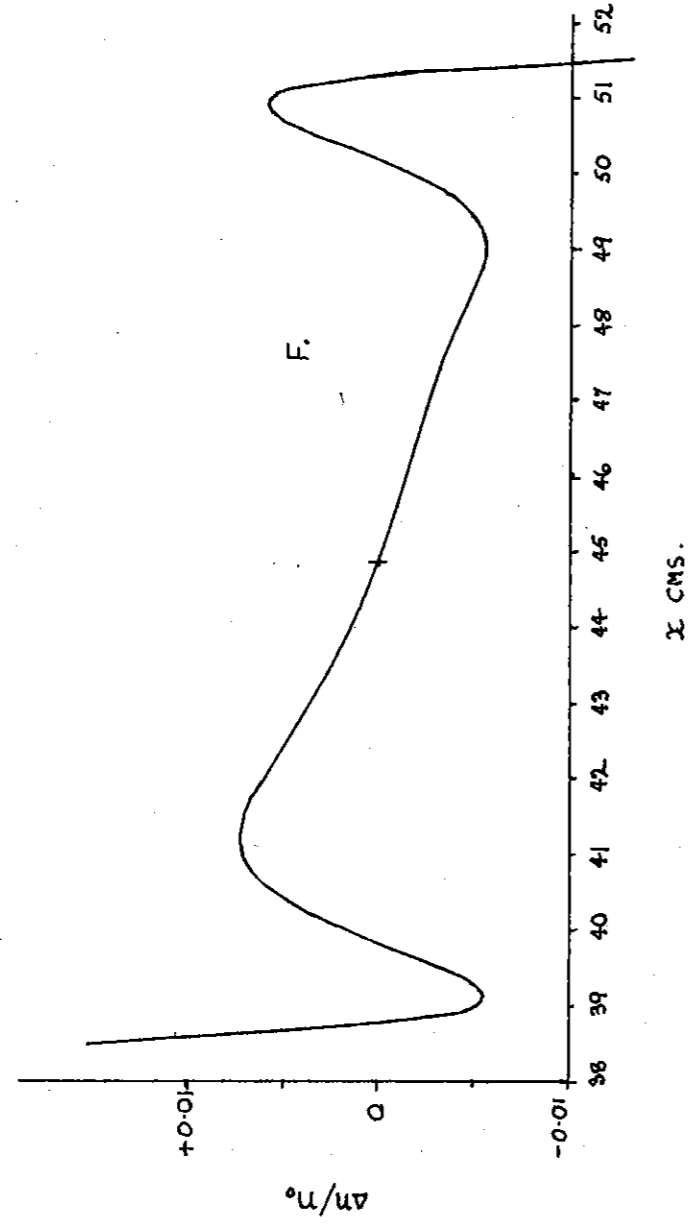


FIG. 1.

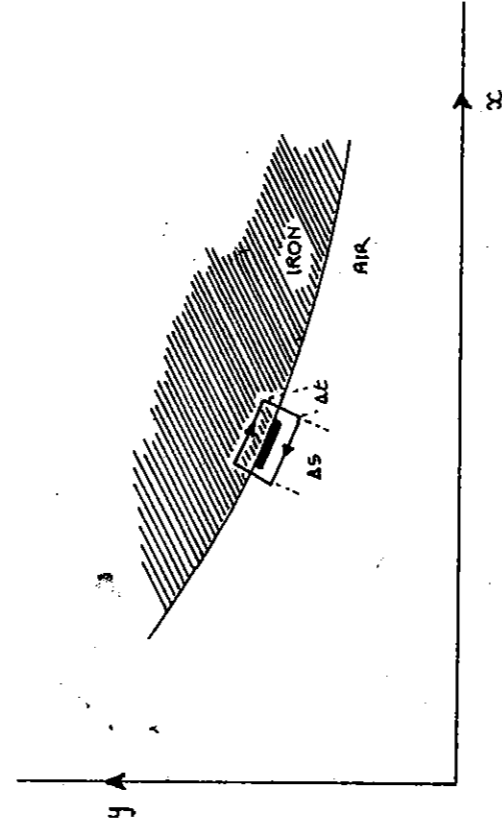


FIG. 2.

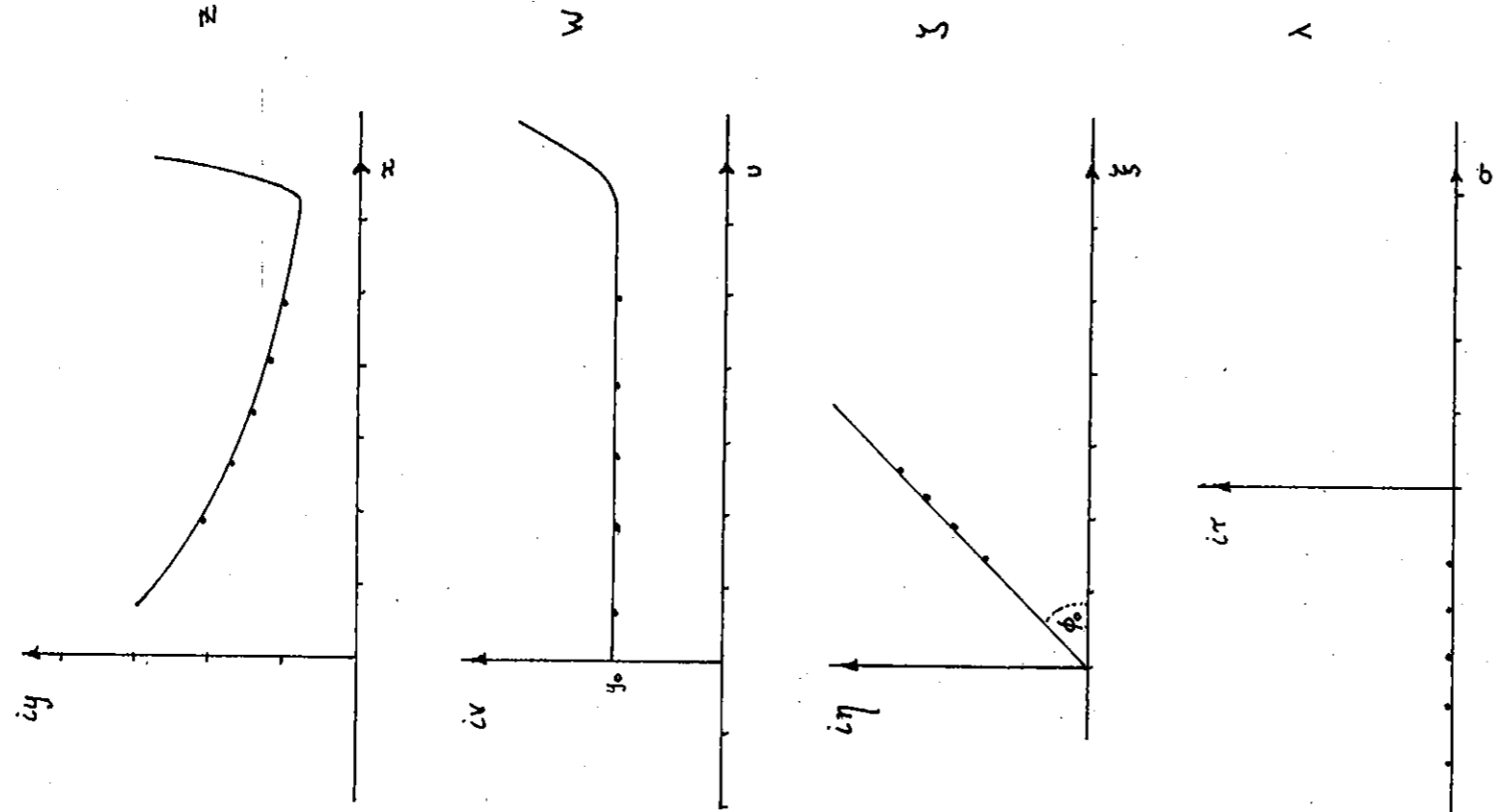
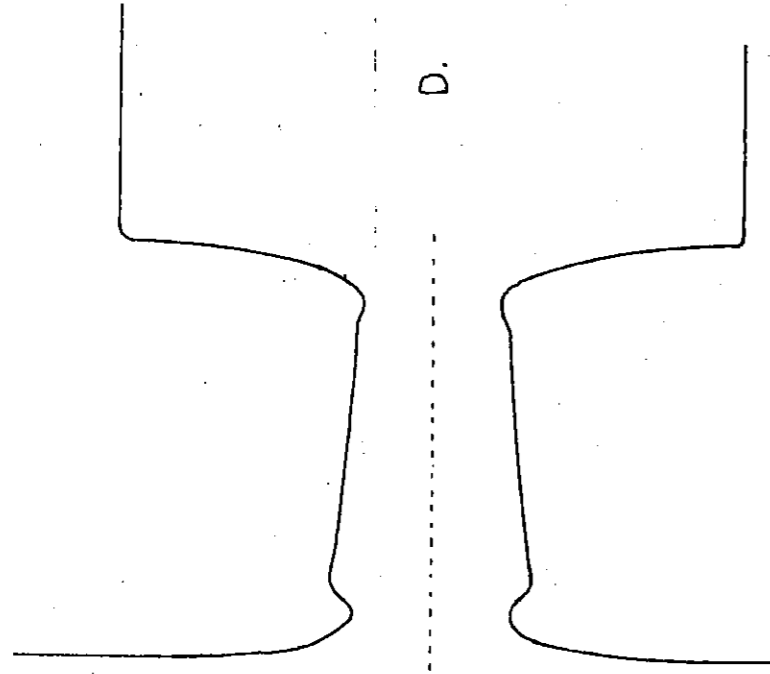
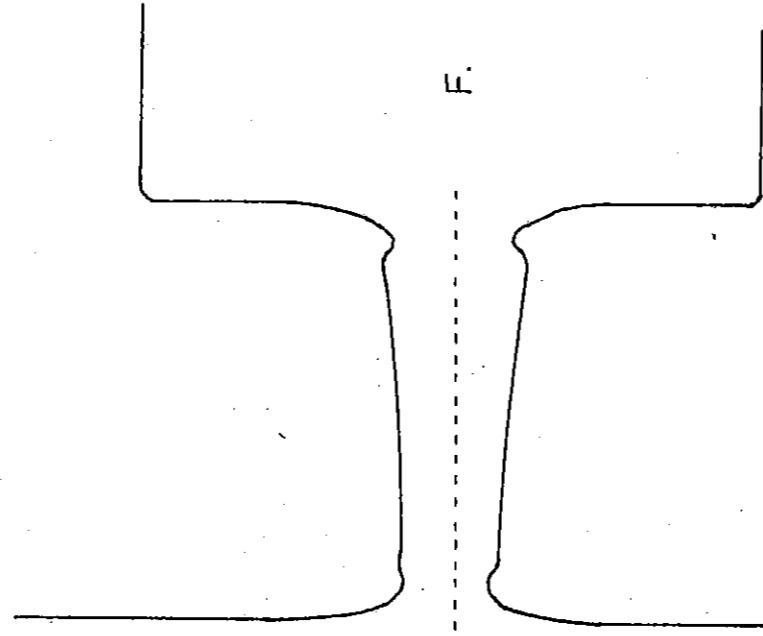


Fig. 3.

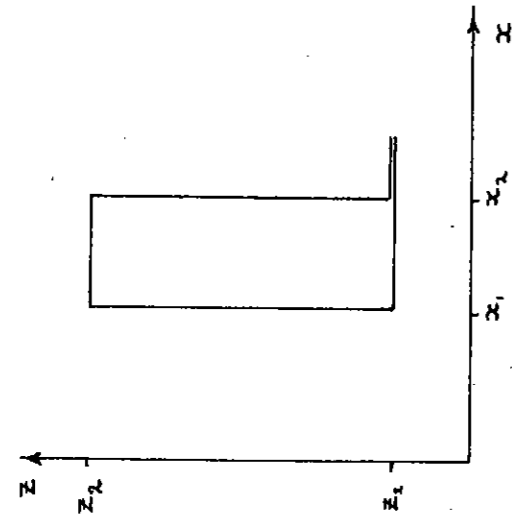


D.

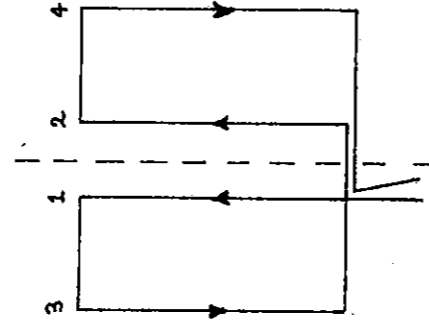


F.

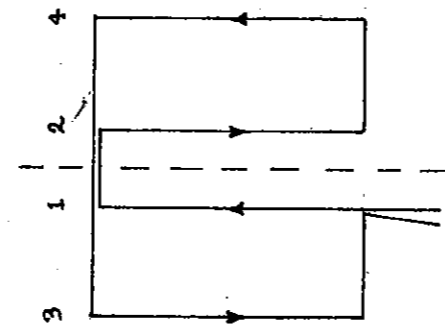
FIG. 4.



5. (a).



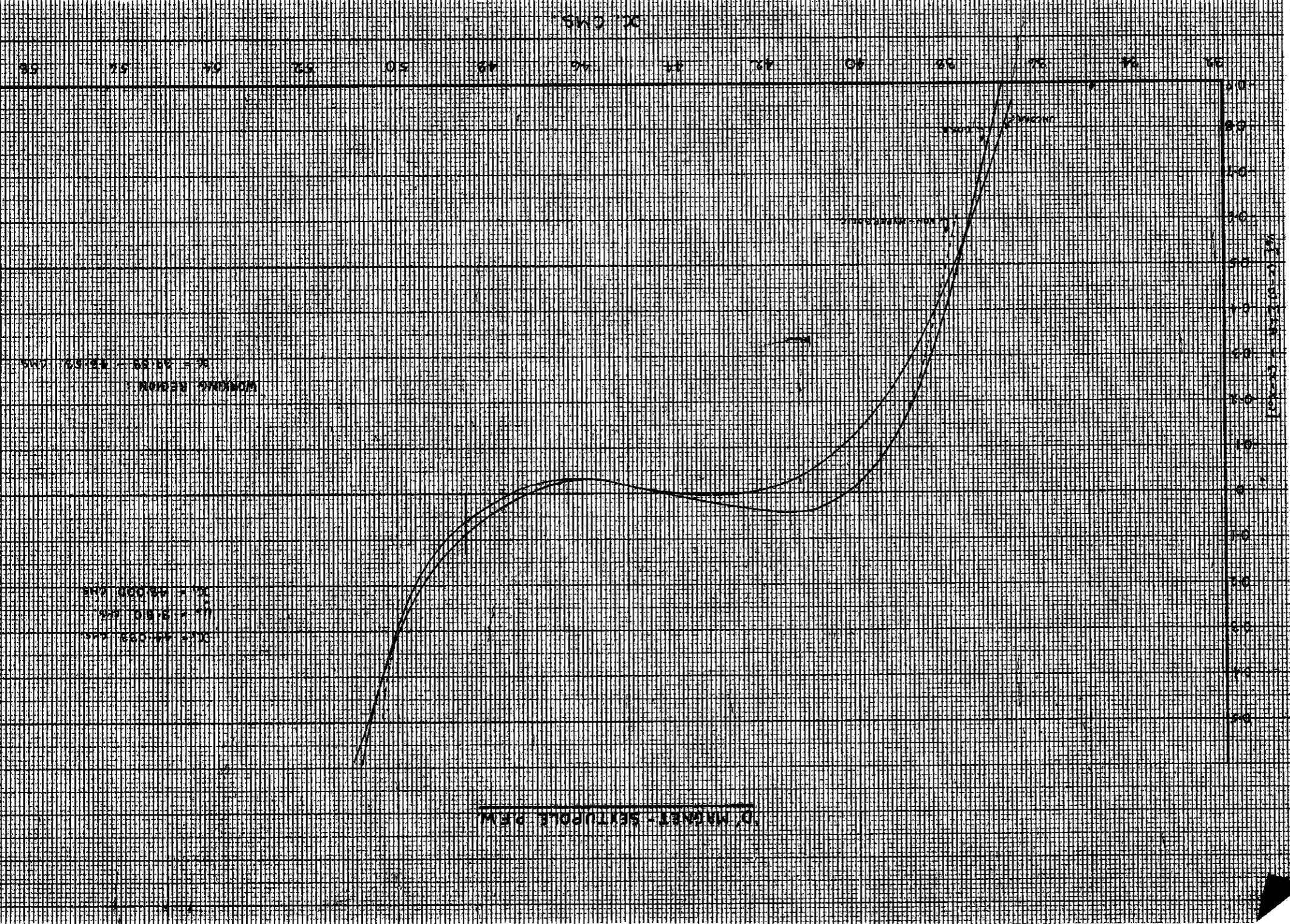
5. (b).



5. (c).

Fig. 5.

FIG. 6.



D. MARGIT - SEITZBOLD, P.M.

X = 0.000 cm
Y = 0.000 cm
Z = 0.000 cm

Wavelength (cm)

X = 0.000 cm
Y = 0.000 cm
Z = 0.000 cm

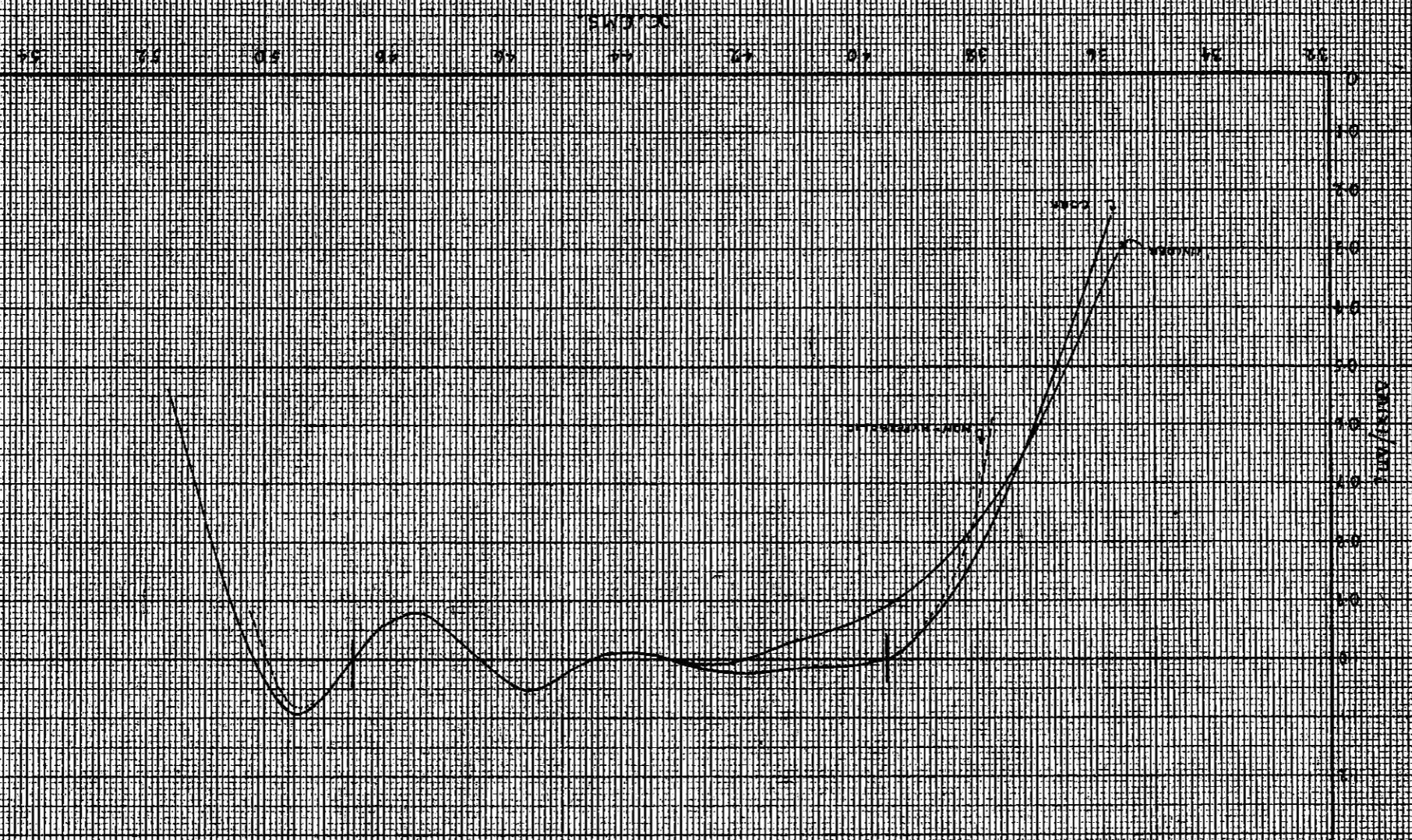
X (cm)

D. MAGNET - QUADRUPOLE FEM

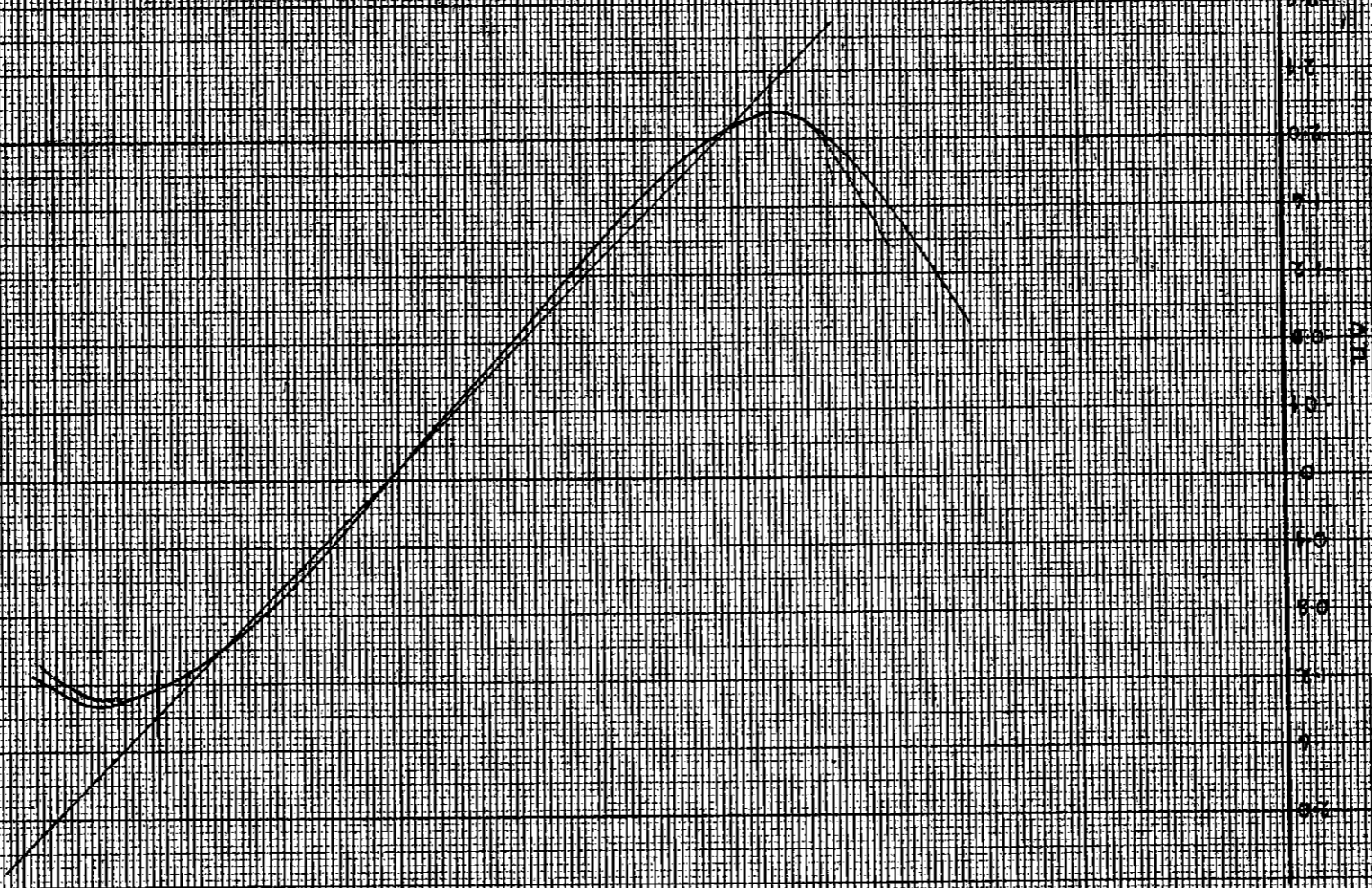
DE = 10000 mm
LE = 10000 mm
ME = 10000 mm

WOLFRAM - RECON
X = 10000 mm

Fig. 1



D'JAGNET - QUADRUPOLE AND SEXTUPOLE



INTEGRATION FIELD = 4.2 GAUSS

QUADRUPOLE: $B_2 = -1.0 \times 10^{-4}$ GAUSS, $B_4 = 0.01$ GAUSS

SEXTUPOLE: $B_6 = 1.0 \times 10^{-4}$ GAUSS, $B_8 = 0.001$ GAUSS

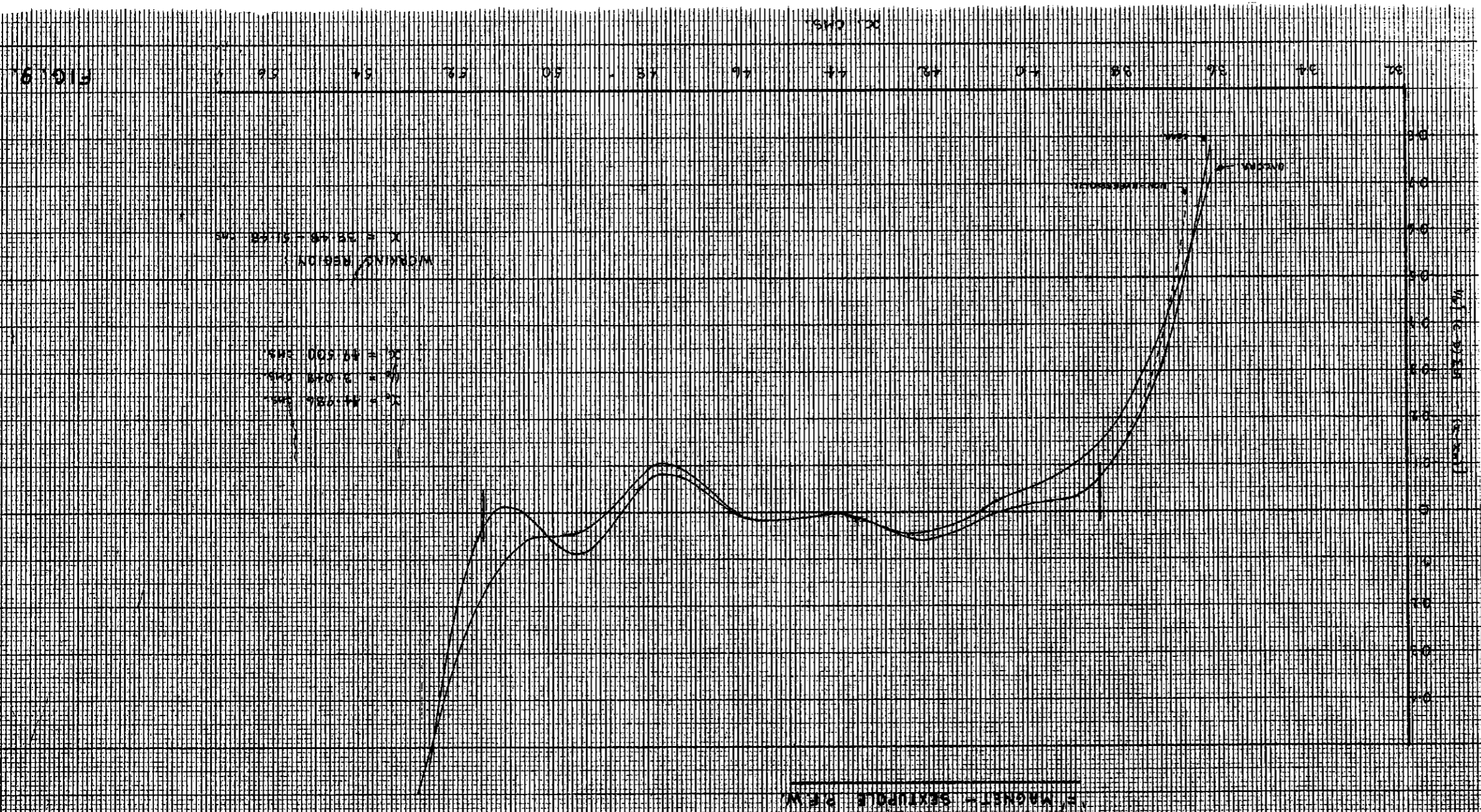
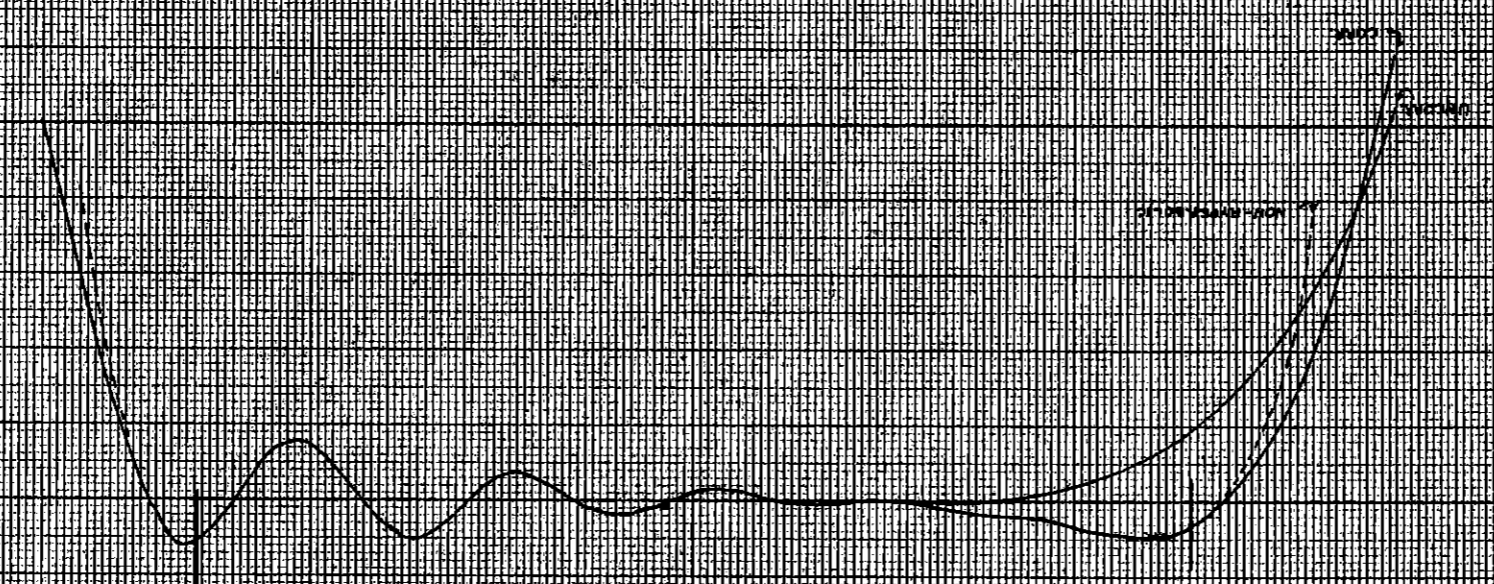


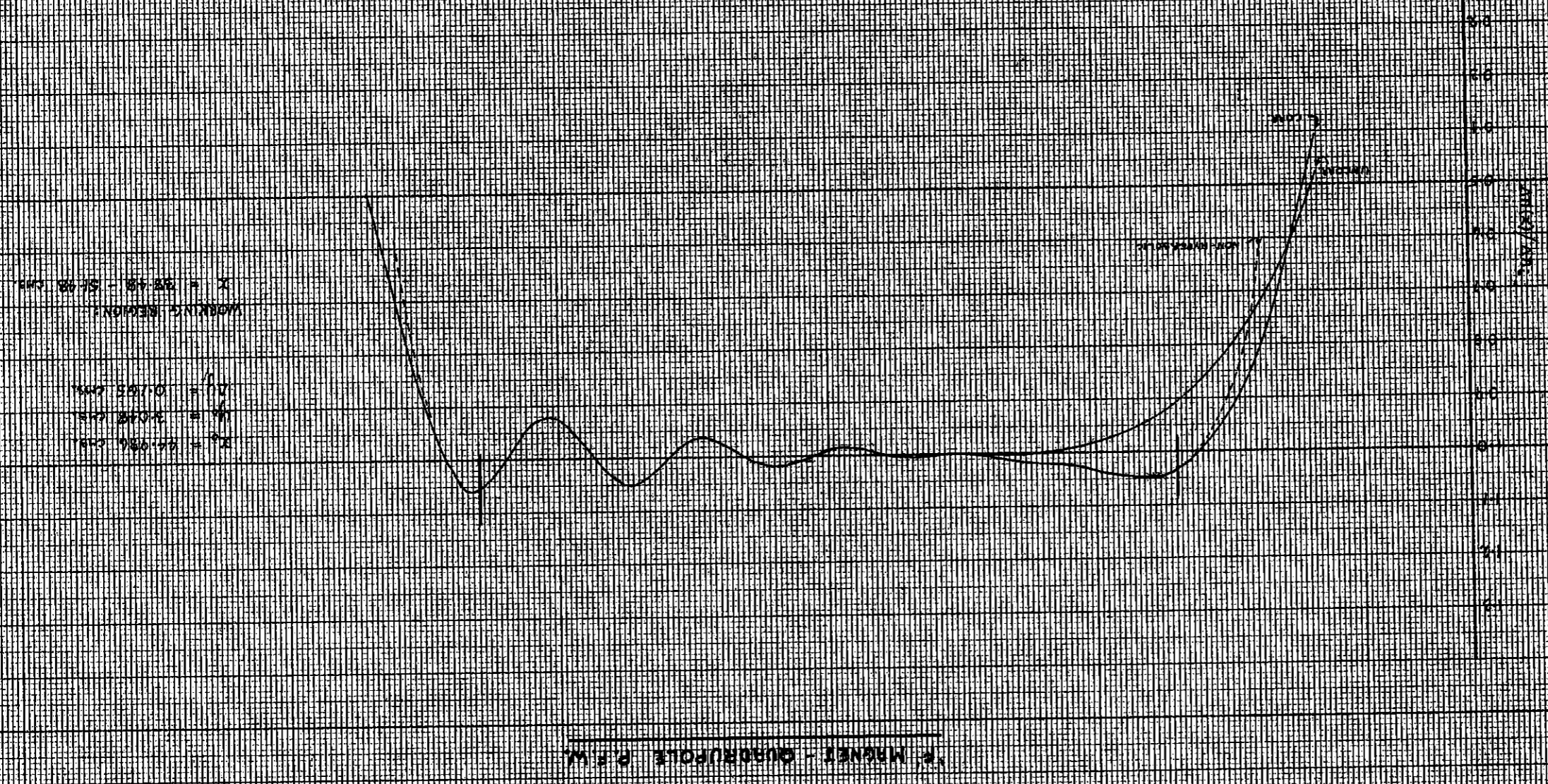
FIG. 10.

$\lambda = 0.0001$
 $\mu = 0.0001$
 $\nu = 0.0001$
 $\rho = 0.0001$
 $\sigma = 0.0001$
 $\tau = 0.0001$
 $\theta = 0.0001$
 $\phi = 0.0001$
 $\chi = 0.0001$
 $\psi = 0.0001$
 $\omega = 0.0001$
 $\delta = 0.0001$
 $\epsilon = 0.0001$
 $\zeta = 0.0001$
 $\eta = 0.0001$
 $\xi = 0.0001$
 $\gamma = 0.0001$
 $\beta = 0.0001$
 $\alpha = 0.0001$



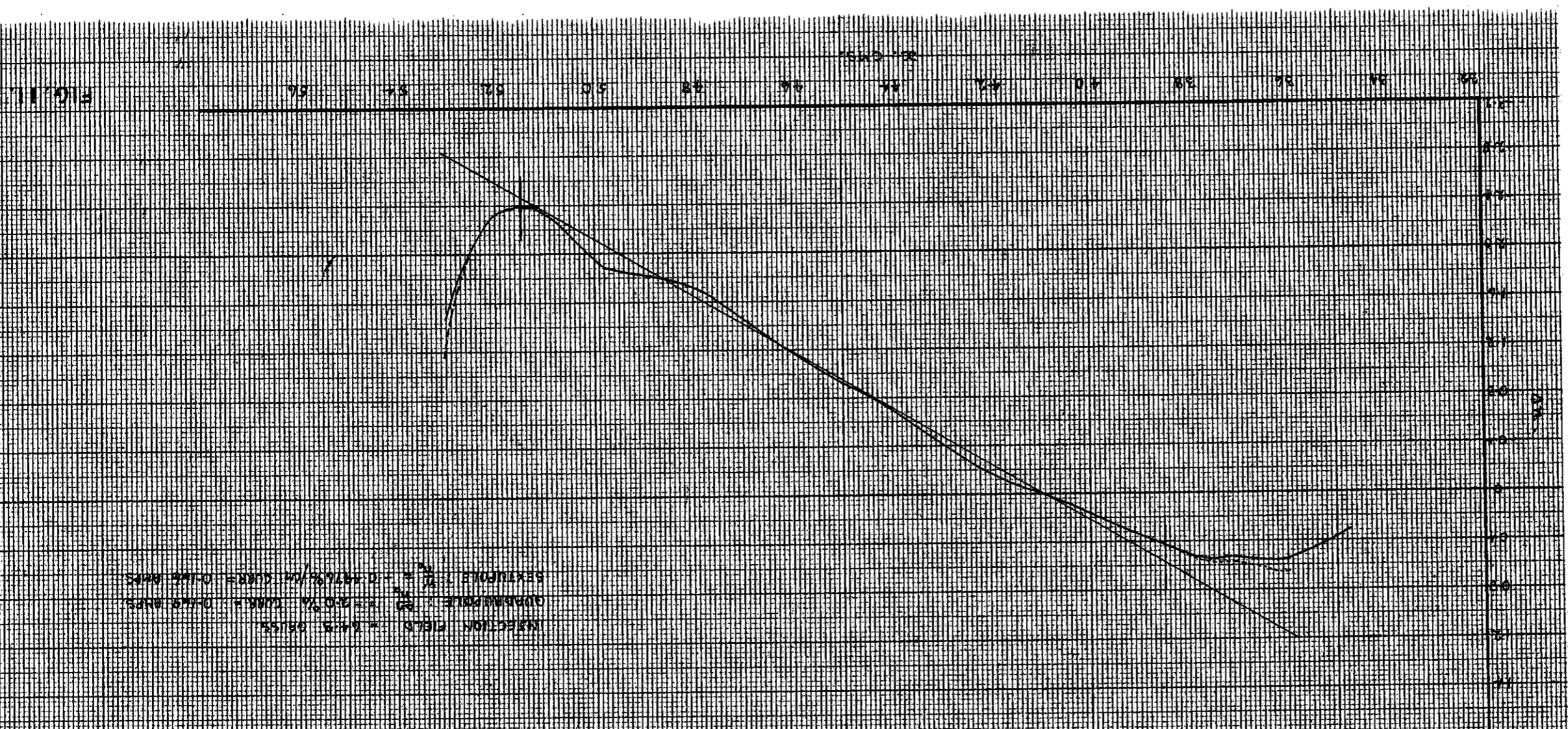
MAGNET - QUADRUPOLE

Fig. 10.



5' MAGNET-QUADRUPOLE AND SEXTUPOLE

MAGNETIC FIELD = 1.15 GAUSS
 QUADRUPOLE = 1.20% TURN/0.15 INCHES
 SEXTUPOLE = 0.471% IN TURN/0.15 INCHES



'D' CONDUCTOR POSITIONS.

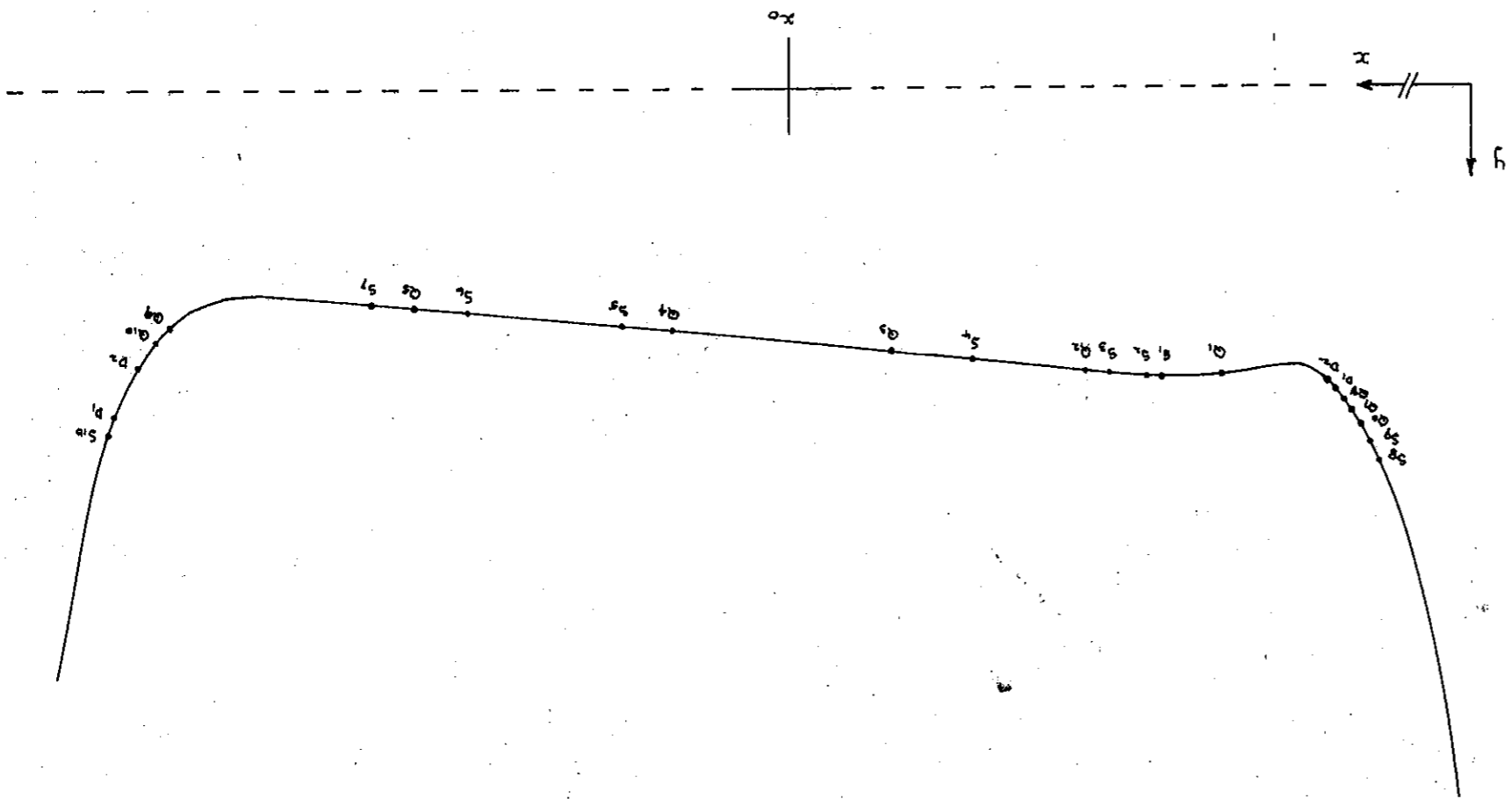


FIG. 12.

F' CONDUCTOR POSITIONS.

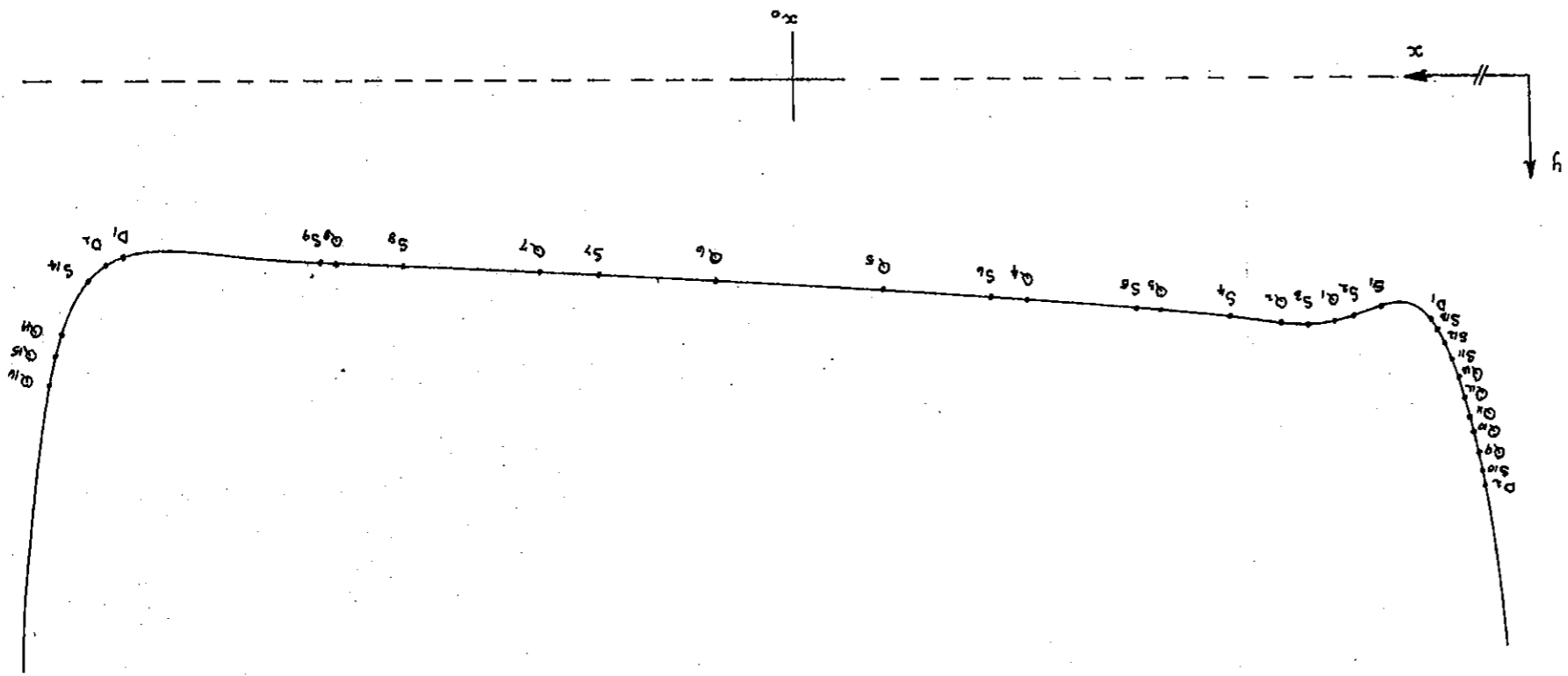
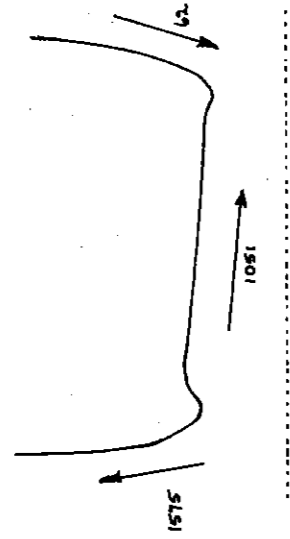
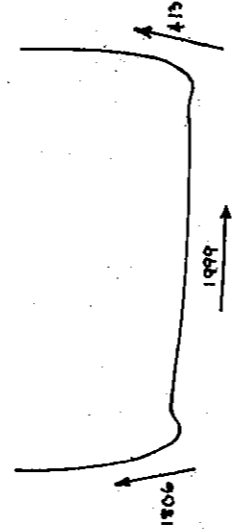
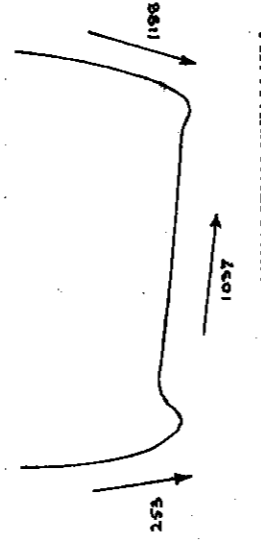


FIG. 13.

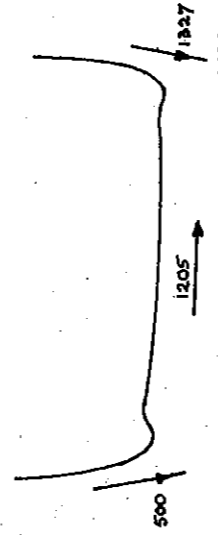
RESULTANT FORCES



D.



E.



FORCES IN GMS. WT.

FIG. 14.